Available online at www.sciencedirect.com
ScienceDirect
Radiation Physics and Chemistry 75 (2006) 2004–2007
Radiation Physics and Chemistry
www.elsevier.com/locate/radphyschem

Bending magnet source: A radiation source for X-ray phase contrast tomography

B.B. Dhal[a,*], A.G. Peele[b], P.J. McMahon[c], F. De Carlo[d], K.A. Nugent[a]

[a]School of Physics, The University of Melbourne, Parkville, VIC 3010, Australia
[b]Department of Physics, Latrobe University, Bundoora, VIC 3086, Australia
[c]Maritime Platforms Division, Defence Science and Technology Organisation, Australia
[d]Advanced Photon Source, Argonne National Laboratory, Argonne, IL 60439, USA

Accepted 4 October 2005

Abstract

The rapid development of electronic data processing and phase retrieval technique for image reconstruction leads to new opportunities in X-ray phase tomography. A range of radiographic and tomographic demonstrations have now been made, typically utilizing the coherent flux from an insertion device at a synchrotron or a micro-focus laboratory source. In this paper we demonstrate that useful results may be obtained using a bending magnet source at a synchrotron. In particular we show that the same beamline can be used to make and characterize a sample made by X-ray lithographic methods.

Keywords: Tomography; Phase; Phase-contrast; Synchrotron; X-rays

1. Introduction

Tomography is a potential imaging technique used to produce high-resolution cross-sectional images of the internal structure of objects. In X-ray phase tomography, these images often represent slices of phase distribution which in turn can be thought as refractive index distribution of materials. Such reconstruction has been of common practice since long by using monochromatic and polychromatic radiation from synchrotron sources usually using the X-ray beam obtained from the insertion devices. We have previously demonstrated quantitative phase imaging using hard X-rays from a bending magnet radiation is possible (Paganin et al., 2000; Nugent et al., 1996), whereas the limiting factor for such investigations were the spatial coherence in the X-ray beam for which a large aperture is required. In this paper, we present 3D-tomographic reconstruction of various samples that represents strong phase contrast but weakly varying refractive indices. Our phase reconstruction results are quantitative in nature. Our results of reconstruction from broad bandwidth allows us considerably reducing the collecting time and has been an effort in the line of real-time tomography attempted by Advanced Photon Source.

There are several techniques that have been implemented that allow the phase variations across the object to be visualized. Examples include: interferometry, Zernike phase contrast, differential interference contrast, segmented detectors or Shack–Hartmann arrays, and diffraction enhanced imaging. These all require the incorporation of some optical apparatus into the

*Corresponding author.
E-mail address: b.dhal@physics.unimelb.edu.au (B.B. Dhal).

0969-806X/$ - see front matter © 2006 Elsevier Ltd. All rights reserved.
doi:10.1016/j.radphyschem.2005.10.038

experiment, which can be difficult in the X-ray context. Another way to visualise the phase variations in the wavefield relies simply on the evolution of contrast in the intensity of the wavefield with propagation. Related approaches has been demonstrated using in-line holography, multiple defocus methods and Wigner deconvolution methods (Chapman, 1996) and optics free propagation method (Snigirev et al., 1996).

Although contrast can be observed, interpreting that contrast in terms of the physical structure in the sample can be difficult. Several methods of inverting the equations governing the propagation of the wavefield have now been developed. These include contrast transfer function methods, which require the assumption of a weak object or of a slowly varying phase with a weakly absorbing object, transport of intensity methods, holographic methods, and far- and near-field iterative methods. In this work we will use a variation of the transport of intensity methods suitable for homogeneous samples in a paraxial wavefield. The reason for this choice is that it is one of only a few analysis methods that can retrieve rapidly varying sample phase using only a single intensity measurement. This makes an experiment simpler to perform and matches the types of sample we were testing.

We investigated two types of samples using tomographic phase imaging; a naturally occurring biological sample (a wasp stinger, probably that of *Vespula germanica*) and some fabricated polymer samples. The fabricated samples were poly methyl methacrylate (PMMA) components made by the process of X-ray lithography. The purpose of our investigation was to demonstrate:

- The utility of bending magnet sources for imaging samples in phase contrast,
- The technique of broad bandpass imaging at a bend magnet source, with the resulting ability to perform extremely fast data collections, and
- The ability of a single beamline to both make and image a sample.

In Section 2, we describe the experimental arrangement and the analysis methods used and in Section 3 we present the results.

2. Experimental arrangement and analysis

The experiments were performed at the bend magnet facility at sector 2 of the Advanced Photon Source at Argonne National Laboratory. The X-ray beam was allowed to pass through the sample and was propagated a distance of 970 mm downstream to a detector and the images were recorded by a CCD camera of effective pixel size of (1.33, 1.66 μm). The detector resolution is the limiting resolution in the imaging system as the demagnified source size for this set up is well submicron. Experimental detail has been described elsewhere (Peele et al., 2005).

We present here the results for four tomographic measurements. The sample descriptions and experimental parameters are shown in Table 1. For each sample projections between 0° and 180° were taken in 0.25° steps. The non-uniform illumination intensity was normalized across the images by dividing through by sample-out images of the beam. These were taken every 20 projections and applied to the corresponding 20 projections to minimize effects of beam instability. In pink beam mode no monochromatisation was used. The bend magnet source beam was modified by a 0.15° reflection from a Chromium mirror and by insertion of 900 μm of Aluminium filters as well as the usual Beryllium windows in the beam line. This produces a net spectrum with significant flux between about 10–30 keV. This had the result of considerably reducing exposure times from the approximately 5 s required for the monochromatic cases. We used an exposure time of 20 ms.

All of the samples considered here are homogeneous in their composition. This makes them amenable to analysis using the following result:

$$T(\mathbf{r}_\perp) = -\frac{1}{\mu}\ln\left[\Im^{-1}\left\{\mu\frac{\Im(I(\mathbf{r}_\perp)/I_0)}{z\delta|\mathbf{k}_\perp|^2+\mu}\right\}\right], \quad (1)$$

where T is the retrieved thickness of the sample, $\mathbf{r}_\perp$ are the transverse coordinates, μ is the linear absorption coefficient of the sample, $\Im^{-1}$ and $\Im$ represent the inverse and forward Fourier transform operators, I is the measured intensity in the detector plane, I_0 is the uniform intensity of the incident radiation, z is the distance from the sample to the detector plane, δ is the decrement from unity of the real part of the refractive index of the sample and $\mathbf{k}_\perp$ are the Fourier conjugate coordinates to $\mathbf{r}_\perp$. For PMMA at 20 keV $\mu = 5.9\times10^{-5}$ and $\delta = 6.7\times10^{-7}$. For the wasp sting we assumed a composition of Keratin with $\mu = 2.78\times10^{-6}$ and $\delta = 2.1\times10^{-8}$ at 13 keV and $\mu = 1.67\times10^{-6}$ and $\delta = 7.4\times10^{-9}$ at 16.9 ± 0.2 keV.

The actual values for the bee sting are not important as we only wish to demonstrate that similar quality

Table 1
Sample and experimental parameters

Sample	CCD pixel resolution (μm)	Energy (keV)
Wasp sting	1.33	13
Wasp sting	1.33	Pink beam
PMMA rotor	1.66	20
PMMA nozzle	1.66	20

results may be obtained using the monochromatic and the broad-band methods. For a non-absorbing object and away from absorption edges, it has been pointed out that in the regime of validity for the transport of intensity solution the detected image is wavelength-independent subject to a wavelength-scaling factor. This means that for a polychromatic source satisfying the same conditions the scaling factor can be replaced by a spectrally weighted sum. Equivalently an appropriate effective wavelength can be used in the analysis. Our wasp sting sample was less than 5% absorbing over the polychromatic spectrum used. It also appears to satisfy the strict TIE validity requirements given some ex post facto knowledge of its structure. We assume that the composition of the wasp sting is akin to Keratin in that there is no major absorption edge structure in the polychromatic band used. The effective wavelength of 16.9 ± 0.2 keV was found by matching the retrieved thickness obtained for the monochromatic case.

The projected images of the samples were normalized to the incident intensity and the projected thickness was retrieved using Eq. (1). The tomographic reconstruction was performed using the radon backprojection method implemented in the Interactive Development Language. The 1024×1024 pixel images were binned into 256×256 images for faster processing. At this resolution tomographic data sets could be processed using a Pentium IV laptop system in a few hours. It should be noted that at the facility where this data was taken it would be possible to reconstruct the tomographic data sets in considerably shorter times by implementing the phase retrieval step and inputting the result into the dedicated processing cluster.

3. Results

Fig. 1(a) and (b) shows the longitudinal view and Fig. 1(c) and (d) shows the lateral view of phase contrast image and the retrieved phase for a projection of a rotor part fabricated in PMMA using X-ray lithography also at the 2BM beamline. The part is 1.1 mm thick with approximately 85 μm slots. The retrieved thickness using Eq. (1) is typically within 10% of this value in the flat parts of the sample. Near the edges the deviations become higher as the TIE validity regime becomes violated near these high gradient areas. Fig. 2(a)–(c) shows some 3D visualizations of the $256 \times 256 \times 256$ tomographic data set. The ability of the method as applied at this bending magnet source to image the features in three dimensions is clearly seen. Fig. 3(a) shows some 3D visualizations of the $256 \times 256 \times 256$ tomographic data set for a lithographically fabricated nozzle part. Again the projected thickness of the sample agrees reasonably well with the actual value. We show a slice from 3D reconstructed PMMA nozzle in Fig. 3(b).

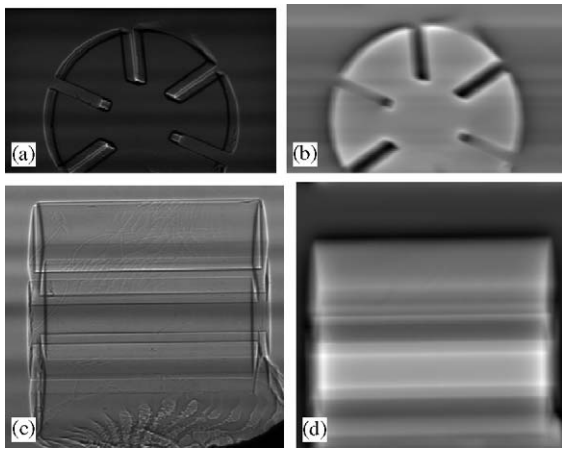

Fig. 1. (a) Phase contrast and (b) retrieved phase image for a lithographically produced PMMA rotor part in longitudinal direction. In (c) and (d) same is displayed along lateral direction.

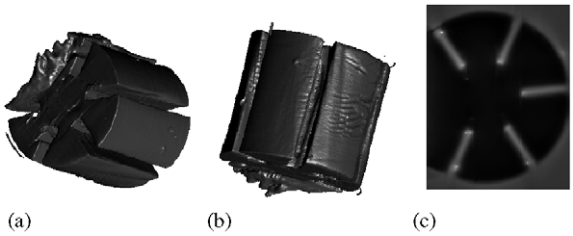

Fig. 2. (a) and (b) 3D view of PMMA rotor, (c) a reconstructed slice of the 3D reconstruction.

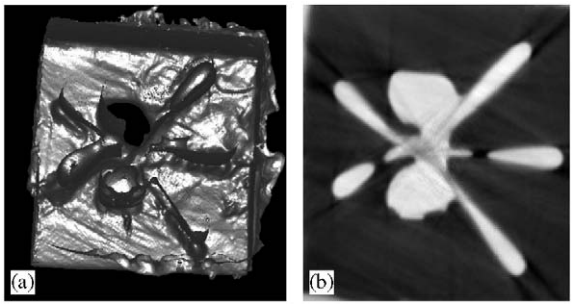

Fig. 3. (a) 3D visualizations of the $256 \times 256 \times 256$ tomographic data set for a lithographically fabricated nozzle part. (b) Displays a reconstructed slice from Fig. 3(a), the projected thickness of the sample agrees reasonably well with the actual value.

The reconstruction shows the clear internal structure of the nozzle voxel.

Fig. 4(a)–(c) shows the upper and lower part of the high resolution 3D image of a wasp sting using the monochromatic beam. This illustrates the detail that can

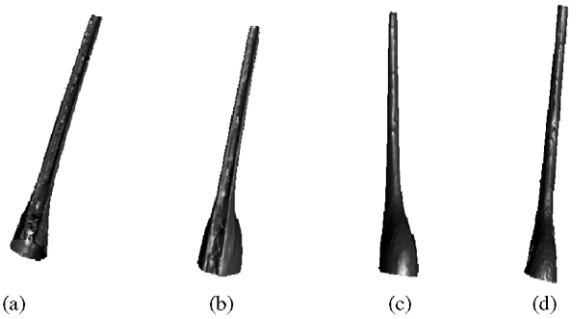

Fig. 4. (a) and (b) lower view of wasp sting reconstructed from by monochromatic (13 keV) and polychromatic illumination, respectively. Fig. 4(c) and (d) represents the same reconstruction showing the upper portion of the wasp sting.

be visualised using these methods. The twin lancets characteristic of the wasp sting are clearly seen as is part of the bulb structure at the top of the sting. Same 3D visualizations are shown in Fig. 4(b) and (d) for polychromatic radiation. It can be seen that the structures retrieved are the same as for the monochromatic case. However, these images were taken in approximately 1/250th of the exposure time as for the monochromatic case.

4. Discussion

Our result demonstrates that a bending magnet source can be used to obtain useful phase contrast images, a fact that appears to have been overlooked in the context of phase retrieval. Competition for insertion device sources remains high and there will be many samples that are admirably matched with bend magnet specifications for phase retrieval. Additionally, we have demonstrated a useful diagnostic tool for beamlines that undertake X-ray lithography. Components so machined can be inspected using the same end-station with only a relatively small additional investment. Furthermore, the PMMA and SU-8 resists commonly used in X-ray lithography will be amenable to the polychromatic methods discussed above. Finally we have shown, using an extremely wide bandwidth that the polychromatic method will work to produce fast phase-retrieved tomographic data sets of a sample. Where less speed is required monochromation systems with broader bandwidth than crystal monochromaters could be used. For instance, a multilayer monochromater ($dE/E \sim 10^{-2}$) has been used for this measurement.

References

Chapman, H.N., 1996. Phase retrieval X-ray microscopy by Wigner distribution deconvolution. Ultramicroscopy 66, 153–158.

Nugent, K.A., Gureyev, T., Cookson, E., Paganin, D., Barnea, D., 1996. Quantitative Phase Imaging Using Hard X-rays. Phys. Rev. Lett. 77, 2961–2964.

Paganin, D., Barty, A., McNulty, I., Frigo, S.P., Wang, S., Retsch, C.C., 2000. Noninterferometric quantitative phase imaging with soft X-rays. J. Opt. Soc. Am. A 17 (10), 1732–1743.

Peele, A.G., DeCarlo, F., McMahon, P.J., Dhal, B.B., Nugent, K.A., 2005. X-ray phase tommography with a bending magnet source. Rev. Sci. Instrum. (in press).

Snigirev, A., Snigireva, I., Kohn, V., Kuznetsov, S., Schlenker, I., 1996. Phase object in synchrotron radiation hard X-ray imaging. J. Phys. D: Appl. Phys. 29, 133–139.